Lawrence Bright, E. S., Springell, R. S., Porter, D., Collins, S., & Lander, G. H. (2019). Synchrotron x-ray scattering of magnetic and electronic structure of UN and U2N3 epitaxial films. *Physical Review B*, *100*, [134426]. https://doi.org/10.1103/PhysRevB.100.134426

Synchrotron x-ray scattering of magnetic and electronic structure of UN and U_2N_3 epitaxial films

E. Lawrence Bright,[1,*] R. Springell,[1] D. G. Porter,[2] S. P. Collins,[2] and G. H. Lander[1]

[1]*School of Physics, University of Bristol, HH Wills Physics Laboratory, Tyndall Avenue, Bristol, BS2 8BS, United Kingdom*

[2]*Diamond Light Source Ltd., Diamond House, Harwell Science and Innovation Campus, Didcot, Oxon OX11 0DE, United Kingdom*

(Received 29 July 2019; revised manuscript received 27 September 2019; published 18 October 2019)

We examine the magnetic ordering of UN and of a closely related nitride, U_2N_3, by preparing thin epitaxial films and using synchrotron x-ray techniques. The magnetic configuration and subsequent coupling to the lattice are key features of the electronic structure. The well-known antiferromagnetic (AF) ordering of UN is confirmed, but the expected accompanying distortion at T_N is not observed. Instead, we propose that the strong magnetoelastic interaction below T_N causes substantial changes in the strain in the sample being measured. These strains vary as a function of the sample form. As a consequence, the accepted AF configuration of UN may be incorrect. In the case of cubic α-U_2N_3, no single crystals have been previously prepared, and we have determined the AF ordering wave vector. The AF T_N is close to that previously reported. In addition, resonant diffraction methods have identified an aspherical quadrupolar charge contribution in U_2N_3 involving the $5f$ electrons.

DOI: 10.1103/PhysRevB.100.134426

I. INTRODUCTION

There is renewed interest in uranium nitride as a so-called advanced-technology fuel to replace the current standard fission fuel, UO_2. This is principally due to its higher thermal conductivity, 20 W/(m-K) at 1000 K [1], compared to ~3.5 W/(m K) for UO_2 [2]. In stark contrast to UO_2, whose thermal conductivity is entirely driven by the phononic behavior, for UN only ~15% is due to any phonon contribution, and the remainder is *electronic* [1]. The ability to calculate these electronic contributions and therefore make predictions about the thermal properties is complex, and attempts have been made by Yin *et al.* [3] and by Szpunar and Szpunar [4], both of which use approximations. In fact, the electronic structure of UN has been controversial for at least 50 years. Despite many studies, even the number of $5f$ electron states, and whether they are localized or itinerant (or some mixture), is still being discussed. The work reported here is thus a contribution to these discussions.

We have recently succeeded in preparing thin epitaxial films [5] of UN and a closely associated material cubic U_2N_3, which is almost always found in conjunction with UN, as it represents a byproduct in the oxidation process. We have also reported the corrosion rates (with H_2O_2) [6] of these materials and found that whereas UN is less corrosive than UO_2, the U_2N_3 material is at least 20 times more corrosive than UN. Since U_2N_3 is found at the surface of UN, this higher corrosion rate is a concern, and our work reported here suggests a possible reason for this difference.

UN has the NaCl *fcc* cubic structure with $a = 4.89$ Å at 300 K. The susceptibility gives an effective moment (μ_{eff}) of ~2.8 μ_B and a large θ_p of ~− 300 K in fitting to the Curie-Weiss law. UN orders antiferromagnetically (AF) at $T_N \sim 53$ K with a type-I AF structure with an ordered moment (μ_{ord}) of 0.75 μ_B [7]. The large discrepancy between μ_{eff} and μ_{ord} and between T_N and θ_p are not understood. Troć *et al.* (2016) [8] have recently given an excellent summary of the properties of UN.

Much less work has been done on U_2N_3, although the structure of the cubic (α form) has been known for many years [9], and is the cubic bixbyite structure common to R_2O_3, where R is a metal atom. The lattice parameter is between 10.6 and 10.7 Å, depending on the exact U/N ratio. Troć (1975) [10] examined the magnetic properties, and the effective moments are around 2 μ_B. The AF ordering temperatures vary as a function of the U/N ratio between 94 K for $UN_{1.50}$ to ~20 K for $UN_{1.72}$. Neither the type of AF magnetic ordering nor the ordered moments are known.

The preparation of such films opens the way for further experimental studies of the properties of both compounds, and thus perhaps a better understanding of the electronic structure, which can then be used in modeling for the thermal conductivity and other properties. In this paper we discuss experiments below room temperature on both UN and U_2N_3 epitaxial films focused on the interaction of the lattice and the magnetic (electronic) structure. This range of temperature is, of course, irrelevant for nuclear fuel applications, but our emphasis is on the electronic structure and how best to describe it.

II. SAMPLE PREPARATION AND EXPERIMENTAL PROCEDURE

Although thin films of UN have been produced before [11–16], they have not been epitaxial but in the best case have been strongly textured [12]. As reported in Ref. [5], we used a sapphire $(1\bar{1}02)$ substrate with a [001]-oriented Nb buffer, and the UN grows on this with a $1{:}\sqrt{2}$ relation and a 45° rotation. The growth temperature of the film was 600 °C, and a 5 nm cap of Nb was deposited at room temperature on the film to prevent oxidation. The film used at the synchrotron had a

*e.lawrencebright@bristol.ac.uk

thickness of 70 nm and a rocking curve of 1.9°. Thin films of U_2N_3 have not been reported previously, and we found these can be grown on CaF_2 substrates ($a_0 = 5.451$ Å) and have a very good mosaic (less than 0.10°) [5] when they are thin. However, for thicker films the mosaic increases, and the 200 nm film we used had a rocking curve of ∼1°. The lattice parameter in the direction of growth is 10.80(1) Å, compared to $2a_0$ (CaF_2) = 10.9 Å, and the in-plane parameters were 10.60(2) Å. Based on the atomic volume, this corresponds to an effective cubic lattice parameter of 10.67 Å, suggesting we are close to stoichiometry [10].

Resonant x-ray scattering (RXS) measurements were conducted at the Materials and Magnetism Beamline I16 at Diamond Light Source [17]. The x-ray energy was tuned to 15 keV ($\lambda = 0.8265$ Å) for sample alignment and determination of the lattice parameter, due to the increased number of reflections available, and to the uranium M_4 edge at 3.726 keV ($\lambda = 3.327$ Å) for measurements of the magnetic diffraction, taking advantage of the resonant enhancement of the magnetic signal. Samples were mounted in a closed-cycle cryocooler for low temperature measurements. A kappa-geometry six-circle diffractometer provides large access to reciprocal space and the capability of azimuthal scans and grazing incidence diffraction. All measurements were performed in vertical geometry, perpendicular to the incident polarization of the beam, and the azimuthal zero reference is taken when the crystal (001) direction intersects the scattering plane. Scattered x rays were measured using either the high-sensitivity Pilatus3-100 K photon-counting area detector or by scattering at ∼90° from a graphite analyzer crystal into a photodiode. Rotating the analyzer crystal about the scattered wave vector provides a measurement of the polarization of the diffracted signal.

III. RESULTS AND DISCUSSION

A. Structural properties of UN films

Figure 1 shows the variation of the lattice parameters in the UN film as a function of temperature measuring higher-order Bragg reflections. The values given by Marples (1970) [18], measured from a polycrystalline sample, are shown as inverted triangles. From this it can be seen that our UN films are slightly *expanded* by ∼0.004 Å (∼7×10^{-4} in terms of strain) in the growth direction due to the interaction with the buffer and substrate. The lattice linear expansion coefficient from 100–300 K is approximately the same as that reported in Ref. [18], but from the in-plane lattice components we can see that the film is under tensile strain of $\sim +20 \times 10^{-6}$, where the growth axis is larger than the mean of the in-plane parameters. Moreover, this strain increases with temperature, as the expansion of the sapphire substrate (indicated by dashed lines in the figure) is smaller than that of UN.

A further point to make here is to note the *expansion* of the lattice below the AF ordering temperature (T_N). This will be considered more carefully below, but it represents an important measure of the interaction of the UN lattice with the magnetic (electronic) components.

Figure 2 focuses on the expansion in the UN lattice when the material orders. We find that our film has $T_N = 45.8(3)$ K, which is lower than the 52–55 K region found in bulk samples

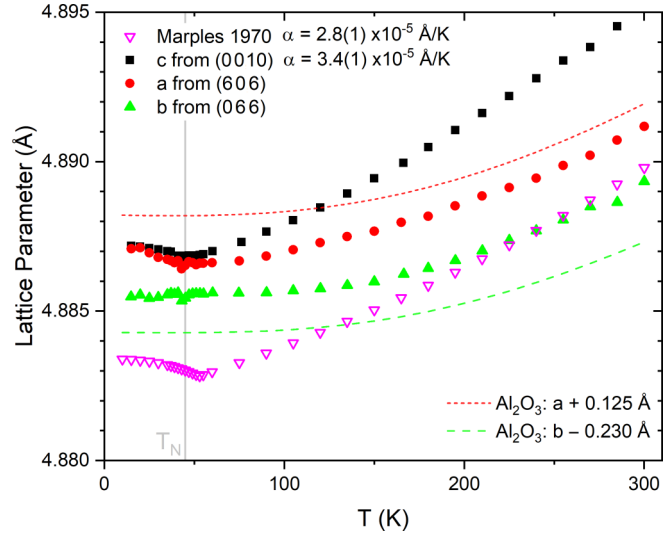

FIG. 1. Lattice parameters as measured from different reflections for the UN film. The values reported by Marples 1970 [18] are given by inverted triangles. c is defined as the lattice parameter in the growth direction of the film. The UN film thickness is 200 nm and the film is deposited on a Nb (001) buffer on a sapphire ($1\bar{1}02$) substrate [5].

[8], and is not surprising given the effect of the strain induced by the substrate. This figure includes data from previous studies [18–21]. Apart from Marples [18], all studies were performed on single crystals, although Refs. [20,21] used strain-gauge techniques, not x rays. What is surprising about this figure is that the expansion of the lattice appears to depend on the sample form, and the magnitude is thus *not* a true bulk property, as it varies by almost a factor of three between different samples. Our results give a lower value, similar to that derived from a polycrystalline sample as measured by Marples [18]. This is particularly interesting, as the study by Shrestha *et al.* [21] shows that this expansion may be partially suppressed by the application of a modest magnetic

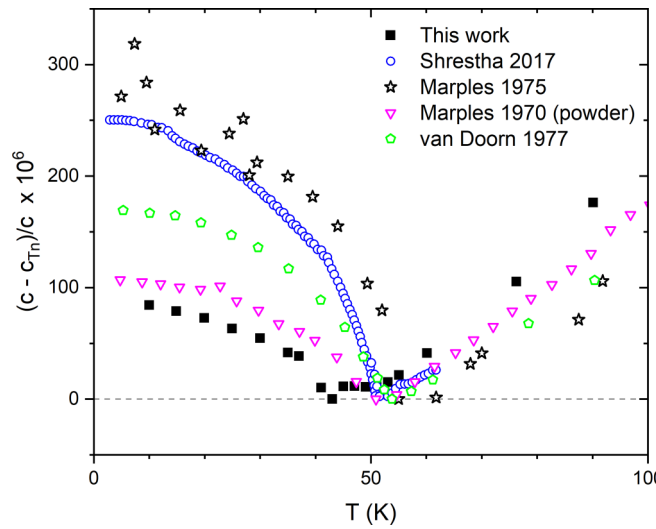

FIG. 2. Relative variation of the lattice parameters in UN below T_N as measured in our work and previously reported in Refs. [18–21].

field (<30 T), although there seems no obvious explanation for this in the AF state. Magnetic fields of ∼60 T are required [8,21] to disrupt the AF order of UN.

We now come to the question of a lattice distortion at T_N. Curry was the first to report the AF structure of UN in 1965 [7]; the structure consists of ferromagnetic sheets of uranium moments arranged in a simple $+-$ orientation along the propagating axis, which, in the single-**k** form, may be any one of the cube axes ⟨100⟩. The moments are parallel to the propagation direction. This immediately gives three possible domains (neglecting time reversal), and the symmetry is *tetragonal*, i.e., one would expect a distortion at T_N so that c (parallel to the propagation direction) is no longer equal to a and b (perpendicular to the propagation direction). However, the possibility of a so-called 3**k** structure, in which all domains exist in one unit cell, cannot be distinguished by the intensities of the reflections, *and this 3***k***configuration has cubic symmetry*. Rossat-Mignod *et al.* [22] were the first to test this on UN and concluded that UN was indeed a 1**k** system, at least under the application of uniaxial stress. They stated that with uniaxial stress UN became tetragonal with $c/a > 1$. Marples *et al.* [19] looked specifically with x-ray diffraction for the expected distortion and reported that $c/a = 0.99935(3)$ at the lowest temperature, i.e., the resulting strain $2(c-a)/(c+a) = 6.5 \times 10^{-4}$. Note this is the *opposite* sign to that suggested in Ref. [22]. A distortion implies that different d spaces will be detected; for example, in the case of the (0 0 10) reflection that the d space for (0 0 10) will be different from that for (10 0 0) and (0 10 0) reflections. A subsequent study, also on a single crystal, by Knott *et al.* [23], found a smaller broadening of the full width at half maximum (FWHM) than reported in Ref. [19] and concluded that the distortion, if present, was smaller than reported in Ref. [19]. There is, therefore, some doubt over the existence of such a tetragonal distortion. It is clear that the behavior of the lattice shown in Fig. 1 needs to be better understood before the question of whether a lattice distortion can be proven. The two phenomena are almost certainly intimately coupled.

Synchrotron x rays have the advantage over laboratory source x rays that there is only one single wavelength and not a mixture (e.g., Cu Kα_1 and Cu Kα_2) in the beam, so we have used this to lower the limit found by samples to a possible strain of $\sim 2 \times 10^{-4}$, as shown in Fig. 3. Unfortunately, Marples *et al.* [19] do not show their raw data of the diffraction profiles, which are simulated in our figure. However, they do show the broadening of the FWHM of their peaks, which they then analyze in terms of a distortion.

However, broadening of the peaks can also be a result of changing strain. This is shown dramatically in Fig. 4, where we show what happens to the FWHM of the (0 0 10) and (555) reflections from the film. The strain along the c axis (growth direction) of the film increases, whereas the corresponding in-plane strain actually compensates by *decreasing*. Clearly, this is a complicated effect, driven by the film-substrate interaction, but it gives no support to the idea of a tetragonal distortion in UN. If that were the case the (555) reflection should not change its FWHM, as all d spaces for this reflection are the same whether a tetragonal distortion occurs or not. Thus, the (555) reflection could change its position but should not broaden; instead it actually narrows its FWHM with decreasing temperature below T_N.

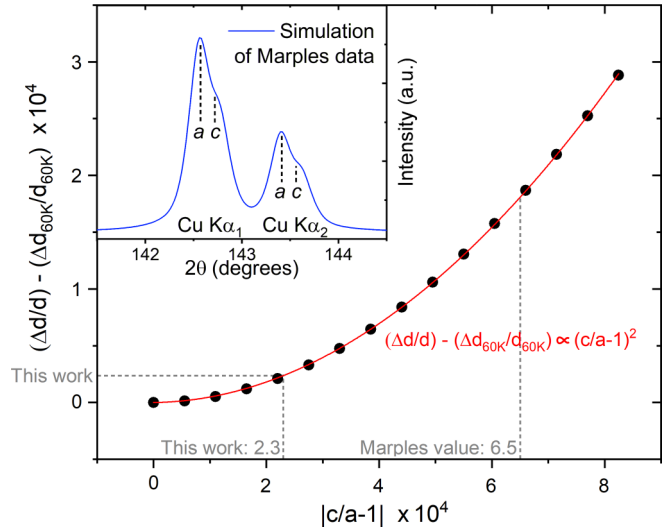

FIG. 3. The relationship between the tetragonal distortion, $|c/a - 1|$, versus the relative change of the FWHM $(\Delta d/d)$ obtained in a simulation for UN. The proportionality factor is 417. The inset shows the profiles that would have been measured by Marples *et al.* (1975) [19] if $(c/a - 1) = 6.5 \times 10^{-4}$. Our data shows that any distortion is smaller, $\leqslant 2.3 \times 10^{-4}$ for $|c/a - 1|$.

The combination of Figs. 2–4 suggests that the tetragonal distortion in UN may not be present without the external perturbation of uniaxial stress and that strain effects in the different samples are more important. It is possible, therefore, that the true state of the magnetic configuration is 3**k**, where a tetragonal distortion would not be expected. The only *unique*

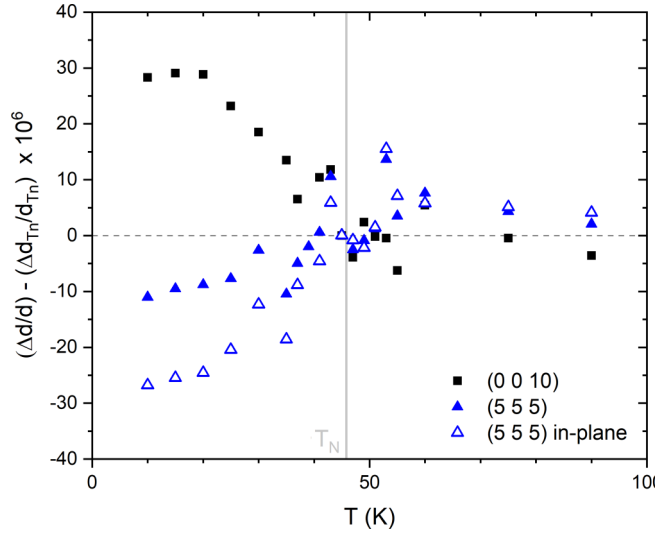

FIG. 4. The relative strain below T_N for the UN film sample in two different directions. The growth direction is given by the (0 0 10) reflection, showing a tensile (expanding) strain as the temperature is lowered below T_N. The in-plane strain (which is compressive in nature) is deduced from combining the results from the (0 0 10) and (555) reflections, and is reduced below T_N. The error bars are $\pm 5 \times 10^6$ units.

way to distinguish these two possibilities is by analysis of the polarization of the spin waves, a complicated neutron inelastic experiment performed only so far for UO_2 [24] and USb [25], both 3**k** systems.

B. Magnetic scattering from UN and U_2N_3 films

1. UN

One of the possibilities with the UN epitaxial film was that the strain in the lattice because of the interaction with the substrate might induce a *single magnetic domain to be observed*. However, below T_N eleven different magnetic reflections (all related by the known magnetic wave vector of $\mathbf{q} = \langle 001 \rangle$) were observed when the energy was changed to the U M_4 edge, and no absences were found. For example in a 1**k** configuration, the (110) belongs to a *c* domain (corresponding to the propagation direction) along [001], whereas the (101) reflection corresponds to a *b* domain, and the (011) to the *a* domain. All were present. Thus the hope that a change in the population of the 1**k** domains might be induced by the substrate-film interaction inducing a slightly orthorhombic UN (as noted in Fig. 1) was not fulfilled. On the other hand, if the true configuration is 3**k**, all such reflections would be present. However, this observation is not *proof* of a 3**k** AF state.

The exact intensity in resonant x-scattering (RXS) is complicated and not related directly to the value of the magnetic moment [26]. The observed intensities depend greatly on the large absorption, which at the U M_4 energy (3.726 keV) in UO_2 can reach values of $\sim 5 \times 10^4$ cm^{-1} [27] corresponding to f'' (the imaginary part of the structure factor) reaching $\sim$70 electrons. In UN this corresponds to a $1/e$ attenuation length of $\sim$150 nm. Some of the beam will pass through the 70 nm film of UN at this energy, but the absorption will depend on the precise geometry and is a difficult correction to make. It is noteworthy that (so far) no report relating *intensities* of magnetic reflections measured at the U M_4 edge has been published. These arguments apply also to U_2N_3 and will not allow the magnetic structure to be determined in that material with this RXS technique. Such an investigation with RXS was reported by Watson *et al.* (1998) [28], but at the L_3 edge of Nd, where the energy is higher than that at the U M_4 edge, and the resonant absorption (i.e., f'') much smaller.

Figure 5 shows the variation of the intensities of magnetic reflections from the two materials as a function of temperature. The reflections are (001) for UN and (003) for U_2N_3. Previous work on bulk UN [29] has given a value of $\beta = 0.31(3)$, and early work on a similar bulk rocksalt uranium compound USb [30] gave a value of 0.32(2). The value determined here, 0.53(5), for UN appears significantly higher. However, there is evidence that critical exponents from thin films are not necessarily the same as those determined from bulk samples. A good example is our recent work on UO_2 [31], where the values for thin films range considerably in value and indicate a second-order phase transition, whereas bulk UO_2 has a first-order transition at T_N. The value found for U_2N_3 is consistent with a simple mean-field model for the transition.

Figure 6 shows the lattice parameters extracted from longitudinal scans of the specular reflections, as a function of

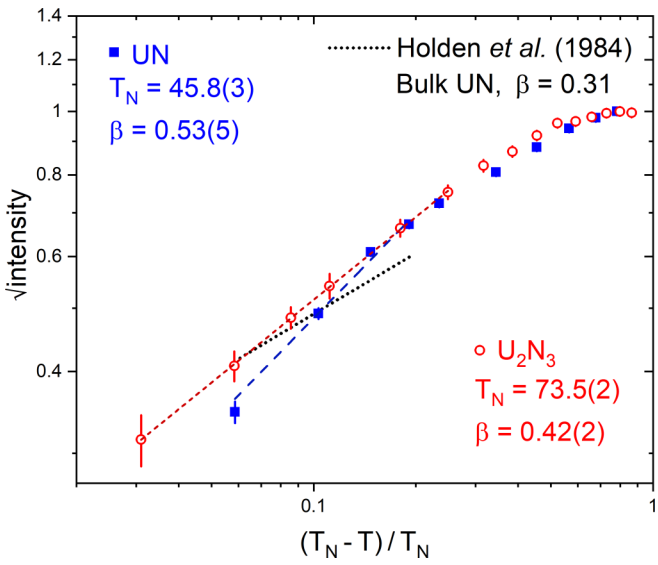

FIG. 5. Plot of the square root of the integrated intensity of the (001) for UN and (003) for U_2N_3 as a function of reduced temperature $t = (T_N - T)/T_N$ on a log-log plot to determine T_N and β. The dotted black line gives $\beta = 0.31$ as determined for bulk UN Ref. [29].

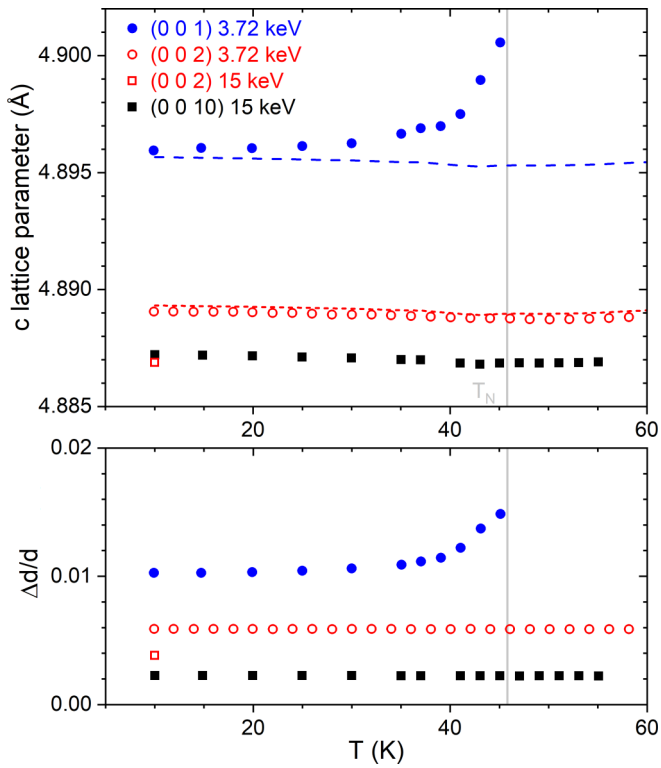

FIG. 6. The lattice parameter *c* and the FWHM ($\Delta d/d$) observed for the various specular peaks as a function of temperature. The large differences in measured *c* lattice parameter, when the energy is shifted from 15 keV to the resonant energy of 3.72 keV, is caused by refraction. The expected values of the (001) and (002) at 3.72 keV, assuming the values at 15 keV are correct, are given as dashed lines using $\delta = 2.0 \times 10^{-4}$, see text.

temperature, together with their *relative* widths $\Delta d/d$. All the reflections taken at 15 keV are in good agreement with one another (as they should be), but lattice parameters measured at the resonant energy appear to be greater. This is due to *refraction effects* and has been known for many years [32]. Normally, these effects are small, but we have an *unusual* case of using relatively long wavelengths x rays, $\lambda = 3.327$ Å, at the U M_4 resonant edge, and the electron density per unit cell, $n_e = 3.41$ electrons/Å^3, is high because of the uranium.

For specular type reflections Greenberg (1989) [33] has shown that Bragg's law can be re-written as

$$\lambda = 2d \sin\theta(1 - \delta/\sin^2\theta), \tag{1}$$

where δ is the correction to the refractive index defined as $n = 1 - \delta$, assuming $n = 1$ in vacuum. This may be readily transformed in the simple case of a specular reflection from sets of planes perpendicular to the growth direction to note that the change in the effective c lattice parameter Δc is given by

$$\Delta c/c = \delta/\sin^2\theta'. \tag{2}$$

$\delta = r_0\lambda^2 n_e/(2\pi)$, where r_0 is the classical electron radius, $r_0 = 2.82 \times 10^{-5}$ Å, giving a value of $\delta = 1.7 \times 10^{-4}$. Normally these values seldom exceed a few parts in 10^{-5}. Here we have also changed θ to θ' to reflect the fact that we are very close to, but not actually at, the specular condition. This is because of the miscut in the substrate. θ' represents the angle between the beam and the surface of the film.

Such effects are much more noticeable for low-angle reflections as the effect is proportional to $1/\sin^2\theta$, which implies [given the almost linear relationship for the low-angle reflections between the reflections (00L) and $\sin\theta$ for the Bragg reflections] that the effect for the (001) reflection is ~4 times more pronounced than for the (002). The dashed lines in Fig. 6 show the values derived by assuming that the 15 keV data give the true value, and the refractive index correction has a value of $\delta = 2.0 \times 10^{-4}$. Given the approximations made with the miscut and treatment of absorption at the lower energy, the agreement with calculated value (1.7×10^{-4}) is satisfactory. By comparison for the (0 0 10) reflection using 15 keV x rays, the correction $\Delta c/c \sim 0.15 \times 10^{-4}$, which is smaller than the error bars in Fig. 6.

Finally, we note in Fig. 6 an unusual effect for the *magnetic* (001) reflection as a function of temperature. There appears to be a steady increase in the effective c lattice parameter around T_N, and this is accompanied by a systematic *increase* in the width of the reflections, signifying a decreased correlation length in the critical regime of UN as the sample is warmed through T_N. This shift cannot, of course, be due to refraction, as the wavelength does not change in these measurements. A simple explanation might be that the magnetic correlations become incommensurate with the underlying lattice, but in that case *two* diffraction peaks would be observed. The (001) magnetic peak in UN arises from the reciprocal lattice points (000) $+q_m$ and (002) $-q_m$, where q_m is the magnetic wave vector, and if $|q_m| \neq 1$, then two peaks would be observed, symmetric about the (001) position. There is no sign of two such peaks. Instead we have a small shift (Dq) in the parameter coupling the magnetic Bragg peak to the lattice; it is as if the magnetic correlations are connected to a lattice with a slightly different (larger) spacing.

This unusual effect has been observed previously at the U M_4 edge, Bernhoeft *et al.* (2004) [34], with the compound USb. We shall not discuss this at length here, as Ref. [34] gives a general overview of experiments on various samples and proposes an explanation, albeit complicated, to understand this shift. Subsequent to this work in 2004, an effort was made to see whether the shifts could also be observed with neutron diffraction, where the resolution is not normally as good as with synchrotron x rays. The successful observation with neutrons, Prokes *et al.* (2009) [35], demonstrates that the effect is not related to the surface of the sample, nor is it a property unique to actinide compounds. We note that this effect is always associated with an *increase* in the width of the magnetic diffraction peaks, signifying a reduced correlation length. This may be seen clearly by noting that the upturn in both panels of the (001) position and relative width in Fig. 6 occur near T_N.

2. U_2N_3

The magnetic structure of U_2N_3 has magnetic peaks that appear at 73.5 K (see Fig. 5) in positions in which $h + k + l =$ odd, i.e., they do not overlap with the charge reflections from the *bcc* structure where the $h + k + l =$ even. The magnetic wave vector is $\mathbf{q} = \langle 001 \rangle$. This implies that the uranium atoms related by the *bcc* translation have *oppositely* directed magnetic moments. Figure 7 shows the polarization analysis scans of three different reflections, one magnetic and two charge, along the specular direction [001] of the U_2N_3 film at 10 K. Purely magnetic scattering in this configuration is σ to π, and purely charge scattering is σ to σ.

The bixbyite cubic structure of U_2N_3 also exists with transition metal ions, i.e., α-Mn_2O_3. However, these materials often have crystallographic distortions associated with the ordering [36], for example. Since we have not detected any distortion of the unit cell [note the symmetric shape of the (004) reflection in Fig. 7], it may be more appropriate to consider the trivalent rare-earth systems, e.g., Er_2O_3 and Yb_2O_3, as investigated by Moon *et al.* (1968) [37].

The magnetic structure of U_2N_3 is similar to that found in Yb_2O_3 [37]; reference to Fig. 3 of that paper shows a complex noncollinear magnetic structure with the moments directed along their local symmetry axes. Of course, since Yb_2O_3 orders at 2.25 K, the exchange interactions in U_2N_3 and Yb_2O_3 are clearly different (For a start, Yb_2O_3 is an insulator, U_2N_3 is a semimetal), so there is no reason to expect similar magnetic structures. Normally, ordering temperatures in the actinides are higher than those of isostructural compounds in the rare earths, simply because of the larger spatial extent of the $5f$ electrons in the actinides, and the fact that such electrons often lie close to E_F, whereas the $4f$ electrons of the rare earths lie well below E_F.

C. Energy dependence of scattering from UN and U_2N_3 films

As is well known [26], the magnetic scattering from the E1 dipole term, corresponding to the M edges of uranium and dipole transitions between the filled $3d$ core level and the partially filled U $5f$ shell, can be represented by a complex

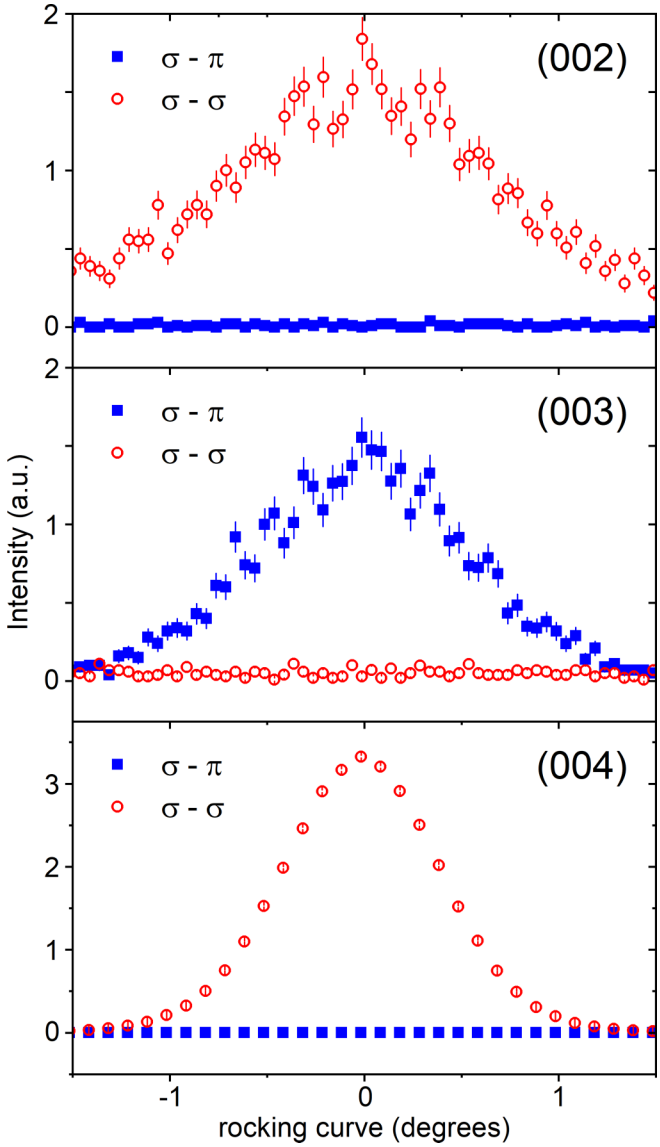

FIG. 7. Polarization dependence of the specular peaks (00L) in U_2N_3 at 10 K measured at the U M_4 resonance energy. The data shows a complete separation between the charge peaks from the *bcc* structure and the magnetic peaks arising from the ordered moments below $T_N = 73$ K. The (002) is a weak reflection; its presence signifies that the positional parameter for the U_2 atom is different from zero. The (003) reflection is magnetic and disappears at T_N.

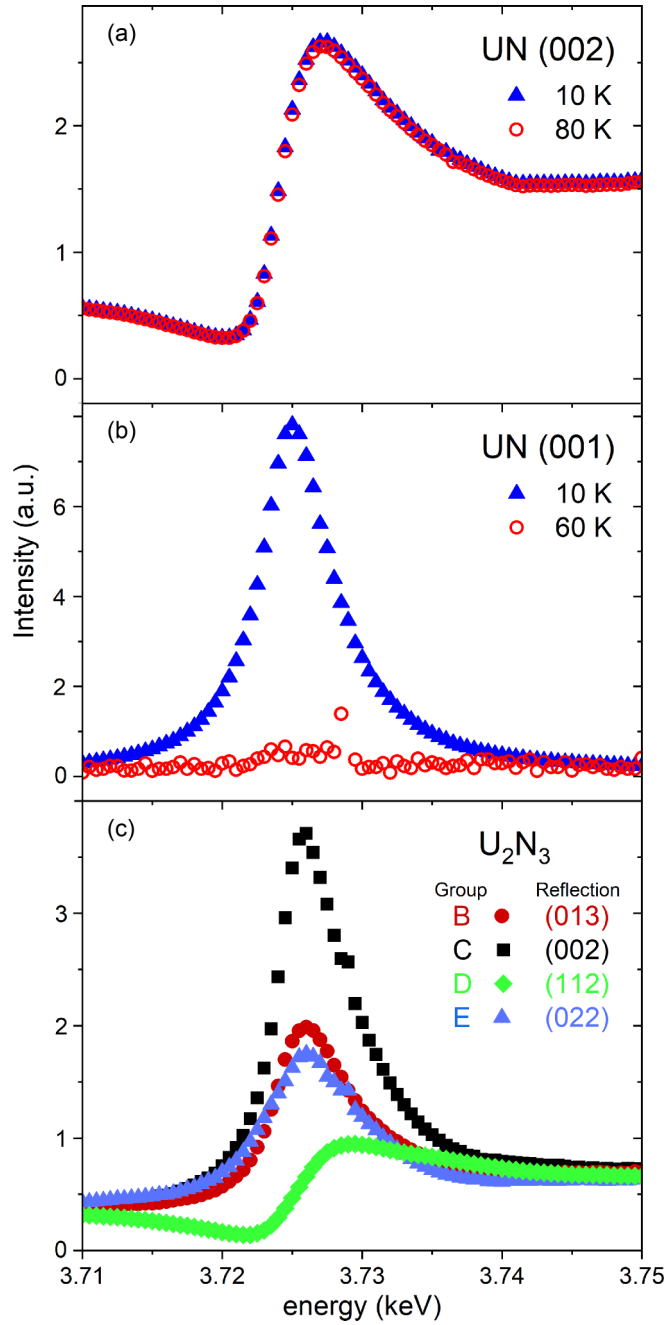

FIG. 8. Energy dependence of the diffraction peaks in both UN and U_2N_3. (a) and (b) show that there is no signal at the (001) of UN at $T = 80$ K ($T > T_N$) and that the energy dependence of the charge (002) does not change with temperature. The bottom panel (c) shows how charge peaks from U_2N_3 vary in energy according to the groups listed in Table I. Groups B, C, and E in U_2N_3 sense the f'' term of the scattering factor, the same term observed in magnetic scattering. Reflections in Groups A (not shown) and D have a standard charge profile in energy through the resonance. These profiles are independent of temperature.

quantity and thus couples to the f'' term of the scattering factor. The imaginary part (related directly to the absorption) is large at the absorption edge. We show in Fig. 8 (top 2 panels) the energy dependence for a charge (002) and magnetic (001) reflection in UN at base temperature. The (002) reflection has a standard charge profile (corresponding to the real part $f_0 + f'$), whereas the *magnetic* (001) reflection has an energy dependence corresponding to the f'' term. The highly symmetric curve with a FWHM ~6 eV is typical for work with thin films [38] and also reflects the partial coherence of synchrotron beam at this energy. Previous experiments on I16 [31] have shown that the energy width can be used to determine whether the film is ordered throughout its depth. In this case the ~6 eV FWHM is expected, so the film is fully ordered.

A key question the experiments above have not answered is whether both uranium sites in the cubic U_2N_3 structure order

TABLE I. Table of structure factors for the first 11 charge reflections in the cubic U_2N_3 structure; space group #206. The cubic lattice parameter used is $a = 10.69$ Å. The quantities SF U_1 and U_2 are the trigonometric structure factors for the uranium atoms for each reflection. No nitrogen atoms are included (there are 48 in the unit cell) and no scattering factor for the U atoms. The reflections in the first column with an x indicate that the reflection is forbidden—group B—whereas group A is with all the atoms in phase and thus a large intensity. The groups are discussed in the text. In the Observation (Obs.) column, Ma and Ch signify magnetic and charge energy profiles, see Fig. 8 lower panel. The final column gives the origin of the ATS structure factor, see text. Reflections indices here follow the convention for cubic systems, $h > k > l$, whereas figures correspond to the observed reflections with the specular direction defined as [001].

(hkl)	$\lvert Q\rvert$ (Å^{-1})	SF U_1	SF U_2	Total SF	Group	Observation	ATS	
(000)	0	8	24	32	A			
(110)x	0.831	0.00	0.00	0.00	B		U_1	U_2
(200)	1.176	−8.00	7.75	−0.25	C	Ma		U_2
(211)	1.440	0.00	1.99	1.99	D	Ch	U_1	U_2
(220)	1.662	8.00	−8.00	0.00	E	Ma		U_2
(310)x	1.859	0.00	0.00	0.00	B	Ma	U_1	U_2
(222)	2.036	−8.00	−23.25	−31.25	A	Ch		
(321)	2.199	0.00	−1.99	−1.99	D		U_1	U_2
(400)	2.351	8.00	23.01	31.01	A	Ch		
(330)x	2.494	0.00	0.00	0.00	B		U_1	U_2
(411)	2.494	0.00	3.85	3.85	D	Ch	U_1	U_2
(420)	2.494	−8.00	6.76	−1.24	C			U_2

magnetically. It would be possible to answer this if we could reliably make the absorption corrections, but this is not the case with a 200 nm film and an absorption attenuation length of about the same order of magnitude, as discussed above.

It is instructive at this stage to consider the geometric structure factors governing the *charge* peaks in U_2N_3, and these are shown in Table I for the first 11 reflections arranged in order of Q, the momentum transfer. In comparing with experiments note that the system is cubic so (hkl) values can be permuted.

There are two uranium sites in U_2N_3, which adopts the structure of the centrosymmetric space group #206. Eight U_1 atoms in the unit cell sit on sites with threefold rotational inversion symmetry (C_{3i}), and twenty-four U_2 atoms sit on sites with twofold rotational symmetry (C_2). There is one adjustable positional parameter for the U_2 sites with positions $(x0\frac{1}{4})$ etc. and none for the U_1 atoms with positions $(\frac{1}{4}\frac{1}{4}\frac{1}{4})$ etc. X-ray [39] and neutron diffraction [40] have been used to determine the positional parameter for U_2 and the consensus value is $x = -0.02$, which we have used in the calculations below. The presence of a finite charge intensity (i.e., σ to σ scattering) at the position (002) [Fig. 7] is direct proof that x for U_2 is not zero.

This table is simply the geometric term in the structure factor *only for the uranium ions*. The 48 N atoms will, of course, contribute to the total intensity, but only by a small amount, and we can neglect this.

Our initial interest in these reflections was in those of group E, where the contributions from the two different U atoms cancel. Of course, this statement is true for the spherical charge density contributions, but aspherical electron distributions, arising from quadrupoles, will stand out after the spherical part cancels. The symmetry elements of both U sites in U_2N_3 allow an interesting phenomenon called anisotropic tensor scattering (ATS) [41,42] to be observed. The symmetry implies that aspherical (quadrupolar) electron distribution may exist around both U sites. A consequence of the reduced symmetry (compared to the very high symmetry observed, for example, in *fcc* UN) is that the local configuration around each U atom may not have an inversion center. This may be seen from Fig. 1 of Ref. [37]. Instead of an eightfold coordination of nitrogen about each actinide ion, there are only six for both the C_{3i} and C_2 sites. The positions of the nitrogen are also marked in Ref. [10], Fig. 7, and these figures also show the noncentrosymmetric local coordination around each U atom. Although such a lack of inversion center may be related to the physical reason the quadrupoles exist, we should emphasize that the symmetry elements alone determine whether this phenomenon can be observed.

The full scattering factor may be written

$$f = f_0 + f' + if'' \tag{3}$$

where the first two terms are real, and the last term is imaginary. The last two terms are zero unless the x-ray wavelength is near an absorption edge. Normally, if the environment of the atom is highly symmetric, the energy dependence of the charge scattering will resemble the well-known dispersive shape, as shown in Fig. 8(a). However, if the spatial dependence of the electronic distribution has an *aspherical* contribution from the quadrupoles, then, with the energy close to an absorption edge this aspherical distribution will couple to f''. Of course, the spherically symmetric part will always be present, so the much smaller asymmetric part cannot be observed unless the spherically symmetric part cancels. U_2N_3 gives a good illustration of this, as shown in the lower part of Fig. 8.

Figure 8(c) shows the energy dependence of various charge reflections allowed in the *bcc* structure of U_2N_3. With reference to the groups listed in Table I, we see that groups B, C, and E sense the imaginary term f'', whereas group D has the real part, $f_0 + f'$, energy dependence. Group A reflections have all contributions in phase and are not sensitive to the aspherical distribution. Group B are forbidden reflections, group C would be zero if $x = 0$ for the U_2 atom, and are thus weak, and group E have the spherical contribution from the two U sites canceling, and are thus also weak. The scattering

from the nitrogen atoms, present in all reflections except group B, is weak compared with any scattering from uranium, so allows the ATS contribution to be also observed in groups C and E.

Previously, ATS scattering has mainly been observed at transition metal K edges [41,42]. However, disentangling the physics from such K-edge measurements is difficult, as the K edge corresponds to $1s$ to np dipole transitions, where n is the first partially filled p shell, and higher-order transitions, (for example, the quadrupole transition is $1s$ to nd) can contribute. In our case, we know that the transitions are dipole in nature and that the aspherical part of the electron density involves the $5f$ electrons, because we observe the effect at the U M_4 edge. To our knowledge no such comparable observation involving $5f$ electrons has been reported previously. To verify that this scattering is truly ATS we have performed an azimuthal scan (not shown) on the (002) reflection, and we have also shown that the ATS scattering of all reflections is independent of temperature. The magnetically-driven ordering of quadrupoles, such as is found in UO_2 and NpO_2 [43], would have a different azimuthal and energy dependence, and is dependent on temperature, with no signal for $T > T_N$.

Table I (final column) shows that there are contributions of the ATS from all reflections from the U_2 atom, but groups C and E have *no* contribution from the U_1 atom. Since we see ATS scattering from group C and E reflections, the aspherical distribution must be present around the U_2 site. Although we cannot exclude its presence around U_1, the fact that the (022) (group E) and (013) (group B) contributions, in Fig. 8(c), are of the *same* magnitude, suggests that any U_1 aspherical contribution is very small, as the (013) has contributions from both U_1 and U_2, whereas the (022) has contributions from only U_2. These two reflections have a Lorentz factor $(1/\sin 2\theta)$ of $\sim$1.2 and are close in $|Q|$. The Lorentz factor for the (002) reflection is 1.71 so it should be stronger than reflections at higher Q. The overall Q dependence for intensities from this dipole transition is still a subject of discussion [26,28].

IV. CONCLUSIONS

A. UN

Early work on UN assumed that the electronic configuration was $5f^2$ and that the $5f$ electrons were localized. Using well-known crystal-field theory, many of the experimental results could be explained on this basis. However, the first neutron inelastic scattering experiments on UN in 1974 failed to find any distinct crystal-field levels [44], and no evidence has been found for such levels in more recent experiments [45,46], so that this theory does not seem immediately relevant. We assume that the crystal-field levels are heavily damped by the interactions between the $5f$ and conduction-electron states. The advent of band theory changed the perspective on even some of the earlier experimental results, in that the orbital moment could be incorporated into such theories [47]. Two important experiments, both on single crystals, added further weight to the idea that the $5f$ electrons are itinerant in UN, firstly, the neutron inelastic scattering [48], and, secondly, the measurement of angular resolved photoemission spectroscopy [49,50].

Although some properties of UN might still be described with localized $5f$ states, giving rise to the idea of duality in UN [8], the weight of evidence points to the best approach being one with band (itinerant) $5f$ electrons. The theoretical calculations mentioned earlier [3,4] both use such assumptions, with the $5f$ states numbering between two and three $5f$ electrons. On the other hand, these calculations do not reproduce the correct (as measured by experiment) AF magnetic moment in UN, and no effort that we are aware of has been made to calculate the ground-state antiferromagnetic state and associated moment, this being an excellent test as to whether the assumed electronic structure is a true representation of the material. When such calculations are made, we can see which of the $1\mathbf{k}$ or $3\mathbf{k}$ magnetic configurations is the more stable state. More complicated is to replicate the *expansion* of the unit cell below T_N, and the effects of the magnetic fields on the system [8,21], which depend crucially on the AF ground state. These large effects with applied magnetic field [51] reflect a strong coupling between spin, electronic, and lattice degrees of freedom.

B. U_2N_3

Although this material is closely linked to UN, very few investigations of its electronic structure have been reported. The crystal structure and its synthesis are well recorded. We have found that our sample orders at 73.5(2) K, with a lattice parameter of 10.80 Å. The magnetic wave vector is $\mathbf{q} = \langle 001 \rangle$, which is the same as that found for Yb_2O_3 [37]. The magnetic configuration may well be noncollinear, but we cannot determine this from our measurements.

In terms of valencies on the individual atomic sites, this is a question that might be answered if we knew whether both sites ordered magnetically. We cannot answer that conclusively with the results of the x-ray experiments reported here. From the U $4f_{7/2}$ spectra reported for U_2N_3 in Ref. [5] there is a shift in the weight of the spectra towards a higher oxidation state than reported for UN. If we assume that the majority 24 U_2 sites are 3+ (i.e., approximately the same as in UN), then charge compensation (taking N^{3-}) suggests the eight U_1 sites might well be of a higher oxidation state, perhaps even U^{6+}. Since U^{6+} is soluble in water and highly reactive, this would explain why the U_2N_3 is more reactive (in H_2O_2) than either UO_2 or UN, as reported in Ref. [6]. U^{6+} would have no associated $5f$ electrons, so would *not* order magnetically, nor should there be any aspherical resonant scattering from U_1 as suggested by the observations in Fig. 8(c). This would be consistent with our observation that the U_1 atom probably has zero (or at least a small) aspherical contribution to the ATS scattering. Of course, such counting of charges is certainly too simple an approach in a material that is certainly a semimetal, and we welcome some theoretical interest given that U_2N_3 is always found in conjunction with (and especially at the surface of) UN.

Similarly, a theoretical investigation should be able to throw light on the ATS scattering reported for U_2N_3 shown in Fig. 8 and believed to be associated only with the U_2 atom. For example, it seems probable that this is related to the hybridization between the U $5f$ states and the N $2p$ states and directly represents $5f$ covalency. Such effects

might be a widespread property of actinide compounds but for its observation requires the special conditions afforded by forbidden reflections in the bixbyite structure [42], which exists for U_2N_3, but not for UN.

ACKNOWLEDGMENTS

We acknowledge Diamond Light Source for time on Beamline I16 under Proposal 20776 and funding from EPSRC Grant No. 1652612.

[1] K. Kurosaki, K. Yano, K. Yamada, M. Uno, and S. Yamanaka, J. Alloys Compd. **311**, 305 (2000).

[2] C. Ronchi, M. Sheindlin, D. Staicu, and M. Kinoshita, J. Nucl. Mater. **327**, 58 (2004).

[3] Q. Yin, A. Kutepov, K. Haule, G. Kotliar, S. Y. Savrasov, and W. E. Pickett, Phys. Rev. B **84**, 195111 (2011).

[4] B. Szpunar and J. A. Szpunar, Int. J. Nucl. Energy **2014**, 178360 (2014).

[5] E. Lawrence Bright, S. Rennie, M. Cattelan, N. A. Fox, D. T. Goddard, and R. Springell, Thin Solid Films **661**, 71 (2018).

[6] E. Lawrence Bright, S. Rennie, A. Siberry, K. Samani, K. Clarke, D. T. Goddard, and R. Springell, J. Nucl. Mater. **518**, 202 (2019).

[7] N. A. Curry, Proc. Phys. Soc. **86**, 1193 (1965).

[8] R. Troć, M. Samsel-Czekała, A. Pikul, A. V. Andreev, D. I. Gorbunov, Y. Skourski, and J. Sznajd, Phys. Rev. B **94**, 224415 (2016).

[9] R. E. Rundle, N. C. Baenziger, A. S. Wilson, and R. A. McDonald, J. Am. Chem. Soc. **70**, 99 (1948).

[10] R. Troc, J. Solid State Chem. **13**, 14 (1975).

[11] L. Black, F. Miserque, T. Gouder, L. Havela, J. Rebizant, and F. Wastin, J. Alloys Compd. **315**, 36 (2001).

[12] D. Rafaja, L. Havela, R. Kužel, F. Wastin, E. Colineau, and T. Gouder, J. Alloys Compd. **386**, 87 (2005).

[13] Y. Zhang, D. Meng, Q. Xu, and Y. Zhang, J. Nucl. Mater. **397**, 31 (2010).

[14] Z. Long, L. Luo, Y. Lu, Y. Hu, K. Liu, and X. Lai, J. Alloys Compd. **664**, 745 (2016).

[15] X. Wang, Z. Long, R. Bin, R. Yang, Q. Pan, F. Li, L. Luo, Y. Hu, and K. Liu, Inorg. Chem. **55**, 10835 (2016).

[16] L. Lu, F. Li, Y. Hu, H. Xiao, B. Bai, Y. Zhang, L. Luo, J. Liu, and K. Liu, J. Nucl. Mater. **480**, 189 (2016).

[17] S. P. Collins, A. Bombardi, A. R. Marshall, J. H. Williams, G. Barlow, A. G. Day, M. R. Pearson, R. J. Woolliscroft, R. D. Walton, G. Beutier *et al.*, AIP Conf. Proc. **1234**, 303 (2010).

[18] J. A. Marples, J. Phys. Chem. Solids **31**, 2431 (1970).

[19] J. A. Marples, C. F. Sampson, F. A. Wedgwood, and M. Kuznietz, J. Phys. C: Solid State Phys. **8**, 708 (1975).

[20] C. F. Doorn and P. D. V. Plessis, J. Low Temp. Phys. **28**, 391 (1977).

[21] K. Shrestha, D. Antonio, M. Jaime, N. Harrison, D. S. Mast, D. Safarik, T. Durakiewicz, J. Griveau, and K. Gofryk, Sci. Rep. **7**, 6642 (2017).

[22] J. Rossat-Mignod, P. Burlet, S. Quezel, and O. Vogt, Physica B+C **102**, 237 (1980).

[23] H. W. Knott, G. H. Lander, M. H. Mueller, and O. Vogt, Phys. Rev. B **21**, 4159 (1980).

[24] E. Blackburn, R. Caciuffo, N. Magnani, P. Santini, P. J. Brown, M. Enderle, and G. H. Lander, Phys. Rev. B **72**, 184411 (2005).

[25] N. Magnani, R. Caciuffo, G. H. Lander, A. Hiess, and L. P. Regnault, J. Phys. Condens. Matter **22**, 116002 (2010).

[26] J. P. Hill and D. F. McMorrow, Acta Cryst. A **52**, 236 (1996).

[27] J. O. Cross, M. Newville, J. J. Rehr, L. B. Sorensen, C. E. Bouldin, G. Watson, T. Gouder, G. H. Lander, and M. I. Bell, Phys. Rev. B **58**, 11215 (1998).

[28] D. Watson, W. J. Nuttall, E. M. Forgan, S.C. Perry, and D. Fort, Phys. Rev. B **57**, R8095(R) (1998).

[29] T. M. Holden, W. J. L. Buyers, E. C. Svensson, and G. H. Lander, Phys. Rev. B **26**, 6227 (1982).

[30] G. H. Lander, S. K. Sinha, D. M. Sparlin, and O. Vogt, Phys. Rev. Lett. **40**, 523 (1978).

[31] Z. Bao, R. Springell, H. C. Walker, H. Leiste, K. Kuebel, R. Prang, G. Nisbet, S. Langridge, R. C. C. Ward, T. Gouder *et al.*, Phys. Rev. B **88**, 134426 (2013).

[32] R. W. James, *The Optical Principle of the Diffraction of X-rays* (Cornell Univ. Press., Ithaca, NY, 1965).

[33] B. Greenberg, Acta Cryst. A **45**, 238 (1989).

[34] N. Bernhoeft, G. H. Lander, M. J. Longfield, S. Langridge, D. Mannix, S. D. Brown, W. J. Nuttall, A. Hiess, C. Vettier, and P. Lejay, J. Phys. Condens. Matter **16**, 3869 (2004).

[35] K. Prokeš, G. H. Lander, and N. Bernhoeft, J. Phys. Condens. Matter **21**, 285402 (2009).

[36] E. Cockayne, I. Levin, H. Wu, and A. Llobet, Phys. Rev. B **87**, 184413 (2013).

[37] R. M. Moon, W. C. Koehler, H. R. Child, and L. J. Raubenheimer, Phys. Rev. **176**, 722 (1968).

[38] N. Bernhoeft, A. Hiess, S. Langridge, A. Stunault, D. Wermeille, C. Vettier, G. H. Lander, M. Huth, M. Jourdan, and H. Adrian, Phys. Rev. Lett. **81**, 3419 (1998).

[39] N. Masaki, H. Tagawa, and T. Tsuji, J. Nucl. Mater. **45**, 230 (1972).

[40] J. Tobisch and W. Hase, Phys. Status Solidi (b) **21** (1967).

[41] S. P. Collins, D. Laundy, and A. Stunault, J. Phys.: Condens. Matter **13**, 1891 (2001).

[42] J. Kokubun and V. E. Dmitrienko, Eur. Phys. J.: Special Topics **208**, 39 (2012).

[43] P. Santini, S. Carretta, G. Amoretti, R. Caciuffo, N. Magnani, and G. H. Lander, Rev. Mod. Phys. **81**, 807 (2009).

[44] F. A. Wedgwood, J. Phys. C: Solid State Phys. **7**, 3203 (1974).

[45] A. A. Aczel, G. E. Granroth, G. J. Macdougall, W. J. L. Buyers, D. L. Abernathy, G. D. Samolyuk, G. M. Stocks, and S. E. Nagler, Nat. Commun. **3**, 1124 (2012).

[46] J. Y. Y. Lin, A. A. Aczel, D. L. Abernathy, S. E. Nagler, W. J. L. Buyers, and G. E. Granroth, Phys. Rev. B **89**, 144302 (2014).

[47] M. S. S. Brooks and P. J. Kelly, Phys. Rev. Lett. **51**, 1708 (1983).

[48] T. M. Holden, W. J. L. Buyers, E. C. Svensson, and G. H. Lander, Phys. Rev. B **30**, 114 (1984).

[49] S. I. Fujimori, T. Ohkochi, T. Okane, Y. Saitoh, A. Fujimori, H. Yamagami, Y. Haga, E. Yamamoto, and Y. Onuki, Phys. Rev. B **86**, 235108 (2012).

[50] S. I. Fujimori, Y. Takeda, T. Okane, Y. Saitoh, A. Fujimori, H. Yamagami, Y. Haga, E. Yamamoto, and Y. Onuki, J. Phys. Soc. Jpn. **85** (2016).

[51] D. I. Gorbunov, T. Nomura, A. A. Zvyagin, M. S. Henriques, A. V. Andreev, Y. Skourski, G. A. Zvyagina, R. Troć, S. Zherlitsyn, and J. Wosnitza, Phys. Rev. B **100**, 024417 (2019).